ACS OMEGA

Open Access

http://pubs.acs.org/journal/acsodf

Article

Antibacterial Coatings of Poly(ethylenimine)/Poly(L-lactide)-Grafted Hyaluronic Acid Multilayers Surface-Functionalized with Bacteriophages

Luise Wirth, Birgit Urban, Eva Bittrich, Gopala-Krishna Mannala, Volker Alt, and Martin Müller*

Cite This: *ACS Omega* 2024, 9, 49432−49440

Read Online

ACCESS | Metrics & More | Article Recommendations | Supporting Information

ABSTRACT: The infestation of tissue after implantation is a major problem as a bacterial biofilm can form on the surface of the implants, leading to implant-associated infections (IAIs). One approach to prevent such IAI is to apply antibacterial coatings consisting of polyelectrolyte multilayers (PEM) and bacteriophages (PHAGs). PEM were constructed by alternately adsorbing oppositely charged polyelectrolytes on a substrate according to the layer-by-layer concept. Poly(ethylenimine) (PEI) was used as the cationic polyelectrolyte, and a graft polymer of hyaluronic acid and poly(L-lactide) (DAC) was used as the anionic polyelectrolyte. Comparing PEM-5 (PEI/DAC/PEI/DAC/PEI) and PEM-6 (PEI/DAC/PEI/DAC/PEI/DAC), a higher amount of PHAG was bound to PEM-5 with cationic surface charge, which was detected by atomic force microscopy (AFM) measurements and attenuated total reflectance-Fourier transform infrared (ATR-FTIR) spectroscopy. The binding of PHAG to the PEM is suggested to be based on electrostatic interactions between the anionic capsid proteins of PHAG and the outermost PEM surface. For antibacterial tests, PEM-5 and PEM-6 each with and without contact to PHAG were deposited at agar plates and infected with bacteria. For the coatings consisting of PEM and PHAG, a significant eradicative effect toward bacteria was obtained, while the pure PEM coatings showed no eradication, which proves the dominant antibacterial contribution originated by PHAG.

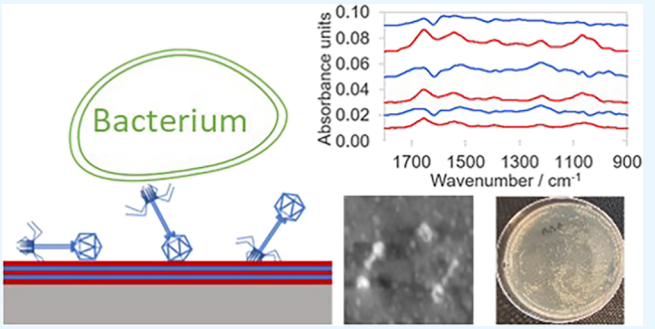

INTRODUCTION

Due to the excessive use of antibiotics in clinical, veterinary, and agricultural settings, antibiotic resistance in bacteria is increasing. Bacterial infections with antibiotic-resistant bacteria are difficult to treat. Hence, it is becoming increasingly important to research alternative therapies against such antibacterial infections.[1] One bacterial strain, where antibiotic resistance has increased significantly in recent years, is the *Staphylococcus aureus* (*S. aureus*),[1−3] which has caused high numbers of hospital-acquired infections. Especially the hospital-germ MRSA (methicillin-resistant *S. aureus*) poses a particular danger when it infects patients with an already weakened immune system.[1] These infections can occur frequently, especially after implantations. When implants are inserted into the human body, the risk of infection with such antibiotic-resistant bacteria is particularly high due to the possible formation of biofilms on the surface of implants. Therefore, implant-associated infections (IAI) with MRSA are a major problem.[1,4,5] Initial bacterial infestation of the implant should be prevented or inhibited at an early stage. Otherwise, a "living" biofilm with uncontrolled multiplication of bacteria will form. Once the biofilm formation reaches a critical level, treatment is almost impossible. Such a bacterial layer on the implant surface protects the bacteria inside from the human immune system and makes treatment with antibiotics more difficult.[2,6,7] One way to treat bacterial infections without the use of antibiotics is bacteriophage therapy.[8] Bacteriophages (PHAG, Figure 1) are the most abundant (micro)organisms on earth (ocean) and were discovered in 1917 by D'Herelle.[8,9] PHAG are rod-shaped viruses that attack and destroy different types of bacteria very specifically and selectively. PHAG specifically acting against a certain type of bacterium can be produced in high amounts by propagating them in this type of bacterium due to replication, transcription, and translation. However, it is difficult to coat implant materials with pure PHAG over a longer period of time as they would be quickly released from the implant material when inserted into the human body. A possible solution to bind PHAG to implant materials is to combine PHAG therapy with polyelectrolyte (PEL)-based surface pretreatment to produce antibacterial coatings.[10,11] For example, polyelectrolyte multilayers (PEM)

Received: July 29, 2024
Revised: November 13, 2024
Accepted: November 18, 2024
Published: December 3, 2024

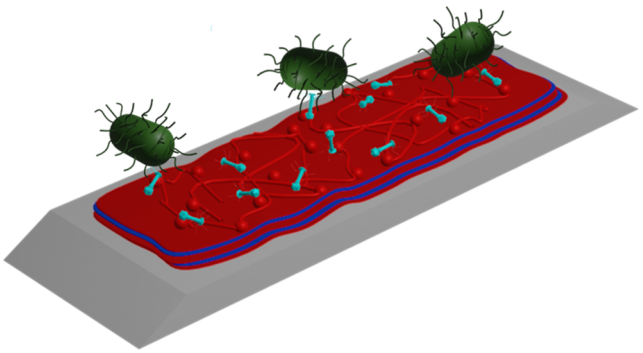

Figure 1. PHAG bound to the outermost layer of a PEM. The PHAG immobilized on the surface protects the surface from bacterial colonization by infecting approaching planktonic bacteria.

consisting of alternating layers of polycations and polyanions can be deposited on a surface using the layer-by-layer concept.[12] The PHAG are expected to interact with the outermost layer of the PEM by electrostatic interactions,[10,13] where the outermost layer of the PEM can have either an anionic terminating layer or a cationic terminating layer, depending on the PEL used. The sketch in Figure 1 shows PHAG bound to the outermost layer of a PEM.

When planktonic bacteria approach, the immobilized PHAG may infect them from the surface. Hence, the PHAG permanently bound to the implant material could serve as prophylaxis by preventing the colony formation of bacteria on the implant surface and thus biofilm formation.[14] Additional antibacterial properties of such PHAG-modified coatings can be achieved using PEL, which are known to have a further specific inhibitory effect on microorganisms.[13] In this work, PHAG were bound to PEM consisting of poly(ethylenimine) (PEI) and an anionic graft polymer of hyaluronic acid and poly(L-lactide), which is commercially available as "defensive antibacterial coating" (DAC). Both cationic PEI and anionic DAC are known to have inherent antibacterial properties.[15,16] Especially, DAC can prevent biofilm formation as it is claimed to represent a physical barrier for bacteria.[16,17] Questions of this study include the effect of the outermost PEL type and amount of bound PHAG on the antibacterial performance of coated model substrates. As substrates, germanium crystals that are easily accessible for interfacial analytical methods and agar plates commonly used for in vitro studies on antibacterial properties were considered.

EXPERIMENTAL METHODS

Substrates. A germanium attenuated total reflectance-Fourier transform infrared (ATR-FTIR) crystal (Ge crystal; 50 mm × 20 mm × 2 mm) was used as a model substrate for polyelectrolyte multilayer (PEM) deposition. The Ge crystal was also used as an internal reflection element (IRE) for ATR-FTIR spectroscopy. PEM was also applied to gold-coated glass substrates, which are quartz crystal microbalance with dissipation (QCM-D) sensors (Biolin Scientific, Gothenburg, Sweden) for QCM-D measurements. Additionally, PEM were applied at standard agar plates, which is further experimentally described below (in vitro antibacterial testing).

Bacteriophages (PHAG). The *S. aureus* lytic virulent PHAG 191219, which is specific for *S. aureus* bacteria, was provided by D&D Pharma GmbH, Pyrmont, Germany. These PHAG were propagated using the *S. aureus* EDCC 5055 bacterial strain, as previously described.[14] Briefly, overnight cultures of *S. aureus* bacteria were subcultured into fresh Luria broth (LB) and incubated on a shaker at 37 °C until reaching an optical density of 1.0 at 600 nm. Subsequently, 5 mL of the PHAG solution, containing PHAG in an amount that resulted in approximately 5×10^8 plaque-forming units (PFU)/mL (see below), was added to 25 mL of bacterial solution and further incubated at 37 °C overnight. The PHAG present in the bacterial suspension were harvested by centrifugation at 4500 rpm for 10 min, followed by filtration of the supernatant through 0.45 and 0.2 μm filters. The titer of the filtered PHAG suspension was determined by using the double agar overlay method.

Polyelectrolyte Multilayer Deposition. The commercial polyelectrolytes (PEL) poly(ethylenimine) (PEI; 25k; 0.01 M; pH 10; Sigma-Aldrich, Darmstadt, Germany; Figure 2a) and

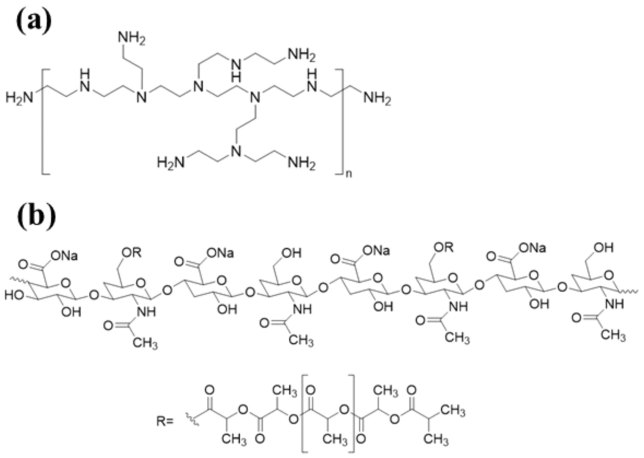

Figure 2. Chemical structures of polyelectrolytes PEI (a) and DAC (b).

hyaluronic acid grafted with poly(L-lactide) (DAC; 0.6 mg/mL; pH 6.2; Novagenit Srl, Mezzolombardo, Italy; Figure 2b) were separately dissolved in Millipore water (18.2 MΩ; Merck Millipore; Darmstadt; Germany) and used for the production of the PEM in all experiments. No further preparation of the solutions was performed.

The PEM were prepared on the germanium (Ge) model substrate in an in situ ATR-FTIR cell by sequential deposition of the PEL. The respective PEL solutions (PEI and DAC) were alternately injected into the in situ ATR-FTIR cell. Each adsorption step was followed by a rinsing step with Millipore water. PEM formation always started with the polycation PEI so that each odd-numbered PEM has a terminating PEI layer, and each even-numbered PEM has a terminating DAC layer. First, approximately 0.5−1 mL of the PEI solution was injected into the in situ ATR-FTIR cell using a syringe, and the solution remained there for 15 min. After this time, the solution was removed, and the cell was then rinsed three times with approximately 1 mL of Millipore water before the polyanion solution was injected into the cell, applying the same residence time as for the PEI solution. This process was repeated as often as required. In each PEL adsorption step, a sublayer of the PEM is formed. PEM-5, for example, consists of the sublayers PEI/DAC/PEI/DAC/PEI. The preparation of PEM was also carried out in the presence of salt. For this purpose, the PEL solutions contained 0.1 M NaCl.

https://doi.org/10.1021/acsomega.4c06933
ACS Omega 2024, 9, 49432−49440

Bacteriophage Adsorption. *S. aureus* PHAG (Uniklinikum Regensburg, Germany, see above) were used in this work. The concentration of the PHAG suspension is related to potential bacterial eradication in a standard process based on agar/bacteria mixtures poured into Petri dishes and quantified in terms of plaque-forming units (PFU), which is a measure for bacterial clearance. According to this, the herein-used *S. aureus* PHAG suspension contained 10^{10} PFU/mL (in LB medium) and was diluted with Millipore water to 10^9 PFU/mL. Adsorption of the PHAG to the PEM was performed by injecting 1 mL of the diluted suspension into an in situ ATR-FTIR sorption cell, where it was contacted with the PEM-coated Ge crystal for 30 min. The PHAG suspension was then removed, and the Ge crystal with the coating was rinsed with Millipore water. Each PEM with adsorption steps between z = 1 and 6 was contacted with the PHAG suspension.

Attenuated Total Reflection-Fourier Transform Infrared (ATR-FTIR) Spectroscopy. ATR-FTIR measurements were performed using a FTIR spectrometer (Vector 22, Bruker Optics GmbH, Ettlingen, Germany) with a special mirror setup (Optispec, Neerach, Switzerland), a globar source, and a mercury cadmium telluride (MCT) detector. The FTIR spectra were measured by collecting 50 scans at a spectral resolution of 2 cm^{-1} (zero filling factor 2) and evaluated using OPUS version 6.5 software from Bruker Optics GmbH, Ettlingen, Germany. In detail, an IRE made of Ge with the dimensions 50 × 20 × 2 mm^3 was installed in an in situ ATR-FTIR cell (M. Müller, IPF Dresden), which contains two chambers sealed by O-rings as reported.[18] The chambers of the in situ cell are located on the upper (sample half) and lower (reference half) halves of the Ge IRE and can be purged with nitrogen or filled with liquids. Both liquids and deposits or adsorbents from these liquids in the wet (contact to water) or dry state can be analyzed by in situ ATR-FTIR spectroscopy.

The surface concentration Γ of deposited compounds can be quantitatively determined by the following modified Lambert–Beer equation:

$$A = \varepsilon \cdot \frac{\Gamma}{d} \cdot d_e \tag{1}$$

where A is the measured absorbance, ε is the absorption coefficient, d is the incremental thickness of the deposited compound layer (from ellipsometry), and d_e is the so-called effective thickness due to Harrick.[19] The effective thickness d_e denotes this thickness of a compound layer, which causes equal absorbance measured by transmission (TRANS)-FTIR spectroscopy (IR radiation transmits the IRE with adjacent compound layer) if compared to ATR-FTIR spectroscopy (IR radiation is internally reflected within the IRE, establishes an evanescent wave at every reflection point, and penetrates into the adjacent compound layer).

Atomic Force Microscopy (AFM). AFM measurements were performed at a Nanostation II (Ultramicroscope, Bruker Nano GmbH, Berlin, Germany), which provides an optical microscope in addition to an atomic force microscope. The SISCANPro software (Bruker Nano GmbH, Karlsruhe, Germany) served as the measurement program. The tips used (r = 10 nm) were from Nanosensors (Darmstadt, Germany). The noncontact mode was used for the measurements. The different PEM layers deposited on the Ge IRE (50 × 20 × 2 mm^3) were measured directly on the latter.

Quartz Crystal Microbalance with Dissipation (QCM-D). The QCM-D analysis of the layer-by-layer buildup and the adsorption of the PHAG was carried out and operated using the QCM-D system Qsense Explorer (Biolin Scientific, Gothenburg, Sweden). As a sensor, a Au-coated crystal (Biolin Scientific, Gothenburg, Sweden) was used. The measurements were performed in a flow. With an automated syringe pump and a flow rate of 0.1 mL/min, the liquids were pumped through the cell. First, the cell was rinsed with Millipore water. Afterward, the layer-by-layer buildup of PEM was setup by alternately pumping the PEL solutions through the cell, with an adsorption time of 15 min for each PEL. Between each PEL adsorption step, it was rinsed with Millipore water for 5 min. After the formation of PEM-5 or PEM-6, the PHAG suspension (10^9 PFU/mL) was pumped through the cell.

An adsorbed mass on the crystal leads to a decrease in the resonance frequency. The resonance frequency is proportional to the mass change Δm in the model of a rigid surface. The data for the change in resonance frequency Δf of each overtone n (3rd, 5th, 7th, 9th, 11th, 13th overtone) are converted by the Sauerbrey equation (eq 2) into the mass change Δm, where C is the mass sensitive constant,[2021]

$$\Delta f_n = -\Delta \Gamma_n = -\frac{f_n}{2} \Delta D_n = -\frac{1}{C} \sqrt{\frac{n \rho_1 \eta_1}{2 \omega_F}} \tag{2}$$

$$\Delta m = \frac{-C \cdot \Delta f_n}{n} \tag{3}$$

f_n resonance frequency; Γ_n bandwidth; D_n dissipation; n overtone order; ρ_1 density; η_1 viscosity; ω_F angular fundamental resonance frequency.

In Vitro Antibacterial Testing. To test the antibacterial activity of the coatings in vitro, PEM-5 (PEI/DAC/PEI/DAC/PEI) and PEM-6 (PEI/DAC/PEI/DAC/PEI/DAC) were applied to agar plates and, optionally, both were further modified by PHAG (PEM-5 + PHAG, PEM-6 + PHAG). For PEM application at agar plates, 1 mL of the PEL solution was spread on the agar plate by swirling and allowed to remain in contact with the agar plate for 2 min. The PEL solutions were applied alternately, with the starting solution always being PEI. After each PEL adsorption step, the agar plates were rinsed three times with Millipore water. Optionally, 0.5 mL of the diluted PHAG suspension (10^9 PFU/mL) was applied to the last PEL layer on the agar plate for 30 min, and the agar plate was again rinsed three times with Millipore water.

Later, the number of PHAG attached to the PEM was analyzed using the plaque-forming unit (PFU) assay against *S. aureus*. For this, 1 mL of the *S. aureus* bacteria (OD_{600} = 1) was mixed with 5 mL of semisolid LB agar medium and poured onto the surface of the coated LB agar plates. The agar plates were incubated overnight at 37 °C. The results were evaluated by counting the number of PFU as a measure for the number of PHAG, which were attached to the PEM. The percentage of bacterial lawn eradication was determined by using ImageJ analysis software. The agar plates not treated by PHAG were used as negative control (no PFU), while the agar plates treated with pure PHAG were used as positive control (10^7 PFU).

RESULTS AND DISCUSSION

Polyelectrolyte Multilayer Deposition. Polyelectrolyte multilayer (PEM) deposition was performed using the layer-by-layer concept known from Decher.[22] Herein, sequential deposition from solutions of cationic poly(ethylenimine)

https://doi.org/10.1021/acsomega.4c06933
ACS Omega 2024, 9, 49432−49440

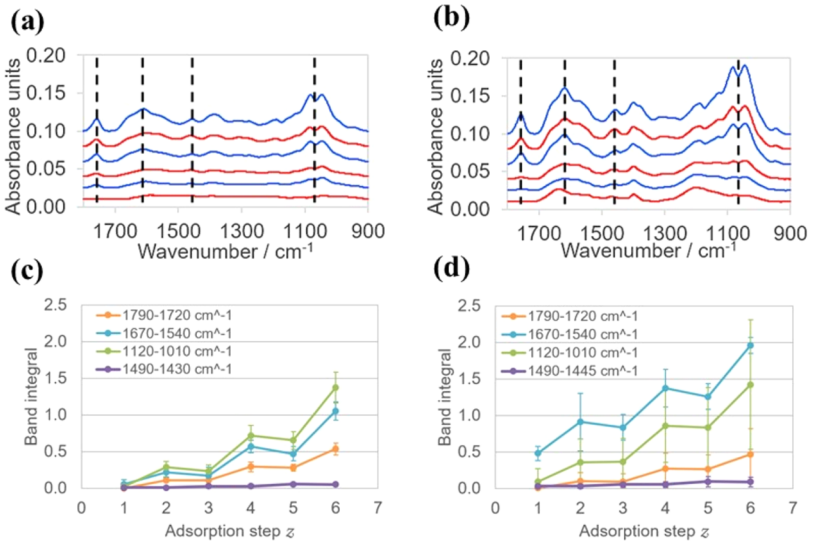

Figure 3. ATR-FTIR spectra on PEM-6 formation by consecutive adsorption of PEI and DAC, prepared without NaCl (a) and with 0.1 M NaCl (b). Integrals of characteristic IR bands of the polyanion DAC plotted against the adsorption step z for PEM-6 prepared without NaCl (c) and with 0.1 M NaCl (d). Error bars are related to standard deviation among triplicates.

(PEI) and anionic lactic acid grafted hyaluronic acid (DAC) on a Ge crystal was applied and studied by ATR-FTIR spectroscopy. The PEM was built up with different numbers of adsorption steps from z = 1 to 6 and in the absence and presence of 0.1 M NaCl. Figure 3 shows the ATR-FTIR spectra on PEM-6 formation for the PEI/DAC system in the absence (a) and presence of 0.1 M NaCl (b).

The IR bands between 1790 and 1720 cm^{-1} (ν(C═O)), 1670−1540 cm^{-1} (amide I/II; IR band around 1620 cm^{-1} due to amide linkage between polylactic acid and hyaluronic acid), and 1120−1020 cm^{-1} (ν(C−O−C)) can be assigned to DAC.

The weak IR band at 1470 cm^{-1} can be assigned to the PEI ($\delta(CH_2)$ bending vibration). In addition, the broad IR band at around 1630 cm^{-1}, which interferes with the δ(O−H) band of water and the amide I band of DAC, might be partly assigned to the δ(N−H) band of PEI. Qualitatively, for both the presence and absence of NaCl, an overall increase of these IR bands is observed after each adsorption step z, indicating layer growth. For quantitative analysis, the integrals of the characteristic IR bands of the polyanion DAC and the polycation PEI were plotted against the adsorption step z, which is given in Figure 3c (no salt) and Figure 3d (0.1 M NaCl).

Generally, based on the amide I/II bands (1670−1540 cm^{-1}) and saccharide band (1120−1010 cm^{-1}), PEM deposition is significantly higher in the presence of salt (Figure 3d) than in the absence of salt (Figure 3c). This result can be explained by the fact that in saline PEL solutions, the charges of the PEL are more shielded so that the PEL are in a more coiled conformation, forming a rather "loopy" layer structure with higher layer thicknesses. In the literature, viscosity measurements can be found, which show a diameter of 40 nm for branched PEI without salt and a diameter of 26 nm for PEI with salt (0.1 M NaCl). The reduction of the diameter of PEI in the presence of salt indicates coil formation due to screened charges.[23]

However, the influence of salt on PEM formation is probably more decisive. In the presence of salt, additional layers can be better integrated into the existing PEM due to the lower repulsion of the last adsorbed layer.[24]

Beside this general increase, both deposition profiles (no salt and 0.1 M NaCl) show a zigzag-like feature, where for the even steps, there is a partial increase, while for the odd steps, there is a partial decrease of the DAC-related IR band integrals. In contrast, the zigzag trend of the weak $\delta(CH_2)$ band due to PEI shows an opposite effect, with local maxima for the odd steps. The same trend was already described for PEM formation from PEI and poly(acrylic acid) (PAC).[10] Obviously, in the odd steps, the respective outermost adsorbed DAC is partly pulled out by the present PEI solution. In this context, it is likely that colloidal polyelectrolyte complex (PEC) particles of PEI/DAC could form.[25]

Additionally, QCM-D was used to characterize the deposition of PEM-6 in the absence of salt. In Figure 4, the mass change obtained by QCM-D is plotted against time.

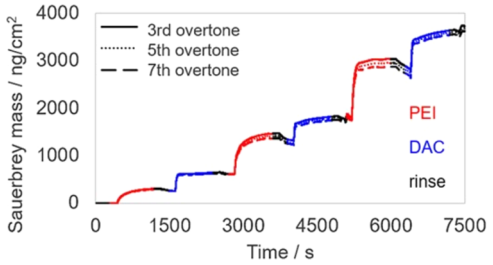

Figure 4. Typical QCM-D data for the consecutive adsorption of PEI/DAC (without NaCl) at the Au substrate.

The changes in frequency for third, fifth, and seventh harmonics versus time were considered and converted by the Sauerbrey equation (eq 2) to the adsorbed mass of PEL (eq 3). Generally, after each adsorption step, a significant increase of mass was obtained, which indicates PEL uptake and PEM formation. Interestingly, for the third (PEM-3) and fifth PEL adsorption step (PEM-5), the incremental mass increase seems to be higher compared to the second (PEM-2), fourth (PEM-4), and sixth (PEM-6) one. Obviously, QCM-D profiles show that during the PEI steps, more PEL material is bound if compared to the DAC steps, while the respective ATR-FTIR

https://doi.org/10.1021/acsomega.4c06933
ACS Omega 2024, 9, 49432−49440

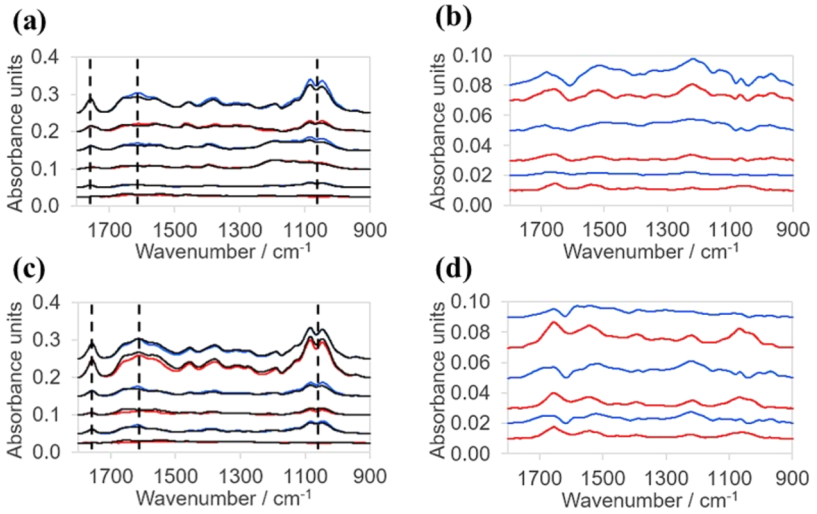

Figure 5. ATR-FTIR-spectra of PEM-1 to PEM-6 prepared without NaCl (a) and with 0.1 M NaCl (c) before (red, terminating PEI layer/blue, terminating DAC layer) and after (black) contact to a PHAG suspension (all after rinsing). ATR-FTIR difference spectra from the subtraction of the IR spectra of the respective PEM without NaCl (b) and with NaCl (d) before PHAG contact from the IR spectra after PHAG contact.

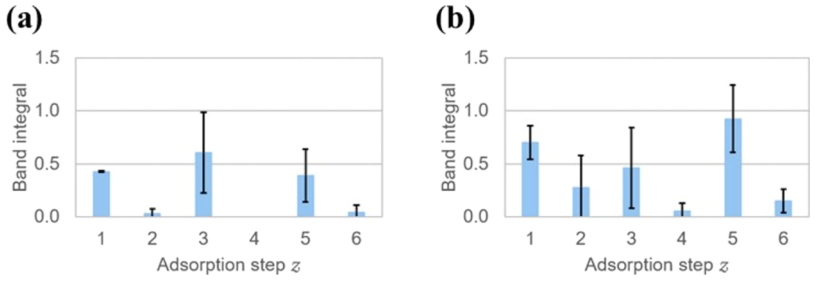

Figure 6. Integrals of amide I and amide II bands (1720−1480 cm^{-1}) from ATR-FTIR difference spectra (Figure 5) plotted against the adsorption step z for PEM without NaCl (a) and with NaCl (b). Error bars are related to standard deviation among triplicates.

profiles show that the DAC amount was partly released. Presumably, there is a readsorption of the formed PEI/DAC complexes resulting in the larger incremental mass increase for the PEI steps, which will not be further addressed herein but in another report. Furthermore, the rinsing step after each PEL adsorption step does not lead to a significant decrease in the adsorbed mass. Hence, the PEL is presumably firmly bound to the surface, and the PEM is stable against rinsing with water, which confirms the ATR-FTIR results.

PHAG Binding at PEM. After showing successful PEM deposition, PHAG were bound at the outermost layer of PEM of PEI/DAC. The PHAG binding was characterized by ATR-FTIR and AFM.

To determine the amount of PHAG bound to the PEM, ATR-FTIR spectra of PEM-1 to PEM-6 before and after contact with the PHAG suspension were recorded. Again, PEM were deposited in the absence and presence of salt. The ATR-FTIR spectra of the PEM before and after PHAG contact (PEM prepared without NaCl (a); PEM prepared with NaCl (c)) as well as difference spectra of these IR spectra (PEM prepared without NaCl (b); PEM prepared with NaCl (d)) are shown in Figure 5.

Furthermore, in Figure 6, the integrated amide band regions between 1720 and 1480 cm^{-1} (obtained in the difference spectra due to the adsorption of the PHAG suspension on the PEM) were plotted against the number of adsorption steps of the PEM. This was done for the PEM in the absence (a) and presence of NaCl (b), respectively.

For the odd-numbered PEM (without NaCl), there is a significant increase in the IR bands around 1630 cm^{-1}, 1550, and 1080 cm^{-1}. These IR bands can be assigned to the amide I (1630 cm^{-1}) and the amide II (1550 cm^{-1}) bands of the capsid proteins of the PHAG. The IR band around 1080 cm^{-1} can be caused either by saccharide moieties of glycoproteins (ν(C−O−C)) or by the phosphate backbone of PHAG DNA (ν(O═P═O)). However, for the even-numbered PEM, no significant increase of these IR bands was obtained. Hence, apparently, deposition of compounds from the PHAG suspension occurs favorably at odd-numbered PEM, while less deposition is found in the even-numbered PEM.

From the literature, it is known that the capsid proteins of PHAG and other viruses have isoelectric points of IEP 2.6−5.2, classifying them as acidic or anionic.[26] Possibly, only the anionic capsid proteins are responsible for binding to the PEM since the envelope formed by the capsid shields the charge of the packed DNA,[27] so that presumably the capsid protein is the major contribution and DNA is the minor contribution. Hence, for odd PEM, this might be caused by electrostatic attraction between anionic capsid proteins and cationic PEI. However, it should be noted that PHAG suspensions in LB medium additionally contain tryptones (protein fragments) and bacterial cell debris (from PHAG production) and may contribute erroneously to the amide I and amide II bands in the IR spectra of Figure 5a,c.

Microscopic PHAG Binding Detection. AFM images of the pure PEM-5 and PEM-6 without PHAG prepared in the

https://doi.org/10.1021/acsomega.4c06933
ACS Omega 2024, 9, 49432−49440

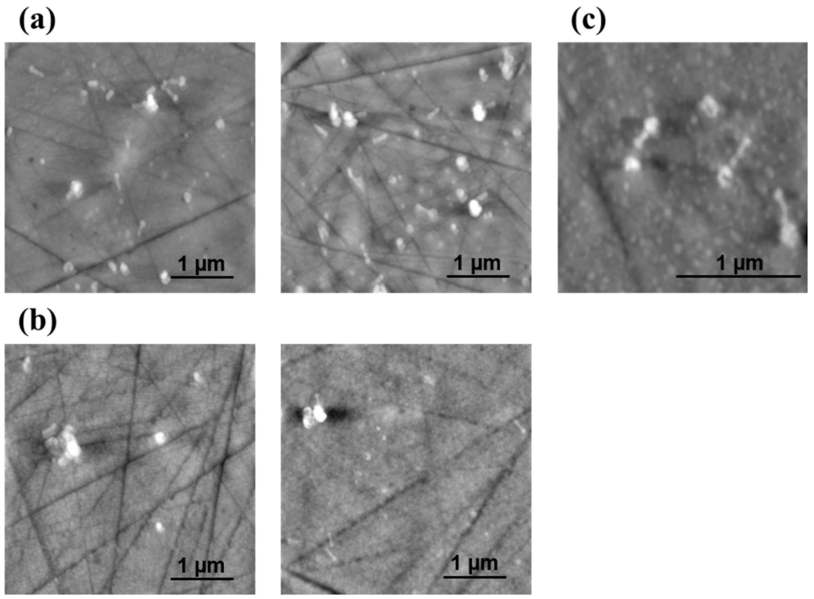

Figure 7. Representative AFM images of two different series of PEM-5 (a, top) and PEM-6 (b, bottom) prepared with 0.1 M NaCl on a Ge crystal after contact to PHAG suspension (scale: 4 × 4 μm^2) and magnified AFM images (scale: 2 × 2 μm^2) of PHAG@PEM-5 (c, right).

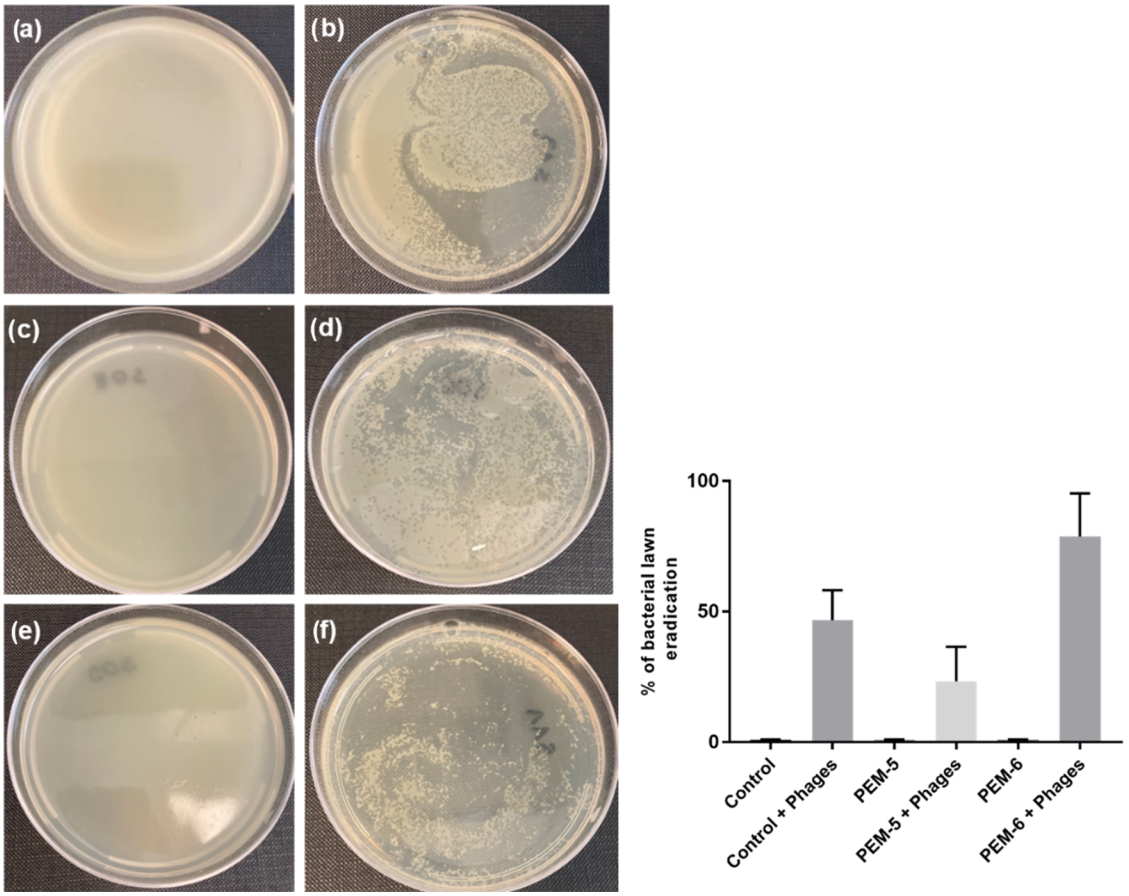

Figure 8. Images of agar plates after infection with *S. aureus* bacteria and incubation at 37 °C. Agar plate as negative control coated with neither PHAG nor PEM (a) and as positive control coated with PHAG only (b). Typical images of agar plates coated with PEM-5 (c) and PEM-5 + PHAG (d) after infection with bacteria and incubation. Typical images of agar plates coated with PEM-6 (e) and PEM-6 + PHAG (f) after infection with bacteria and incubation. Diagram of bacterial lawn eradication (%) for the PEM and PEM + PHAG coatings.

absence of salt (0.1 M NaCl) are shown in Figure S1 of the Supporting Information. For PEM-1 to PEM-6 with PHAG prepared in the absence of salt, generally only a few PHAG-like objects and thus low attachment of PHAG were obtained, which is shown in Figure S2 (Supporting Information). Also only few PHAG were identified in the AFM images of PEM-1

https://doi.org/10.1021/acsomega.4c06933
ACS Omega 2024, 9, 49432−49440

to PEM-4 after contact with the PHAG suspension in the presence of salt (0.1 M NaCl), which are given in Figure S3 (Supporting Information). However, AFM images of PEM-5 and PEM-6 prepared in the presence of salt after contact with the PHAG suspension, as shown in Figure 7, revealed significant numbers of PHAG-like objects.

Significantly, more PHAG-like objects were bound to PEM-5 than to PEM-6. These particular objects show various geometries from spherical to elongated. Spherical particles could either be formed upon complexation of pulled-out PEL and readsorption (see above) of such nanoscopic polyelectrolyte complexes[28] or components of the LB medium like tryptones or cell debris. The elongated particles with characteristic "head−tail-structure" can be assigned to PHAG, and these were also preferentially bound to PEM-5 when compared to PEM-6. The larger amount of attached PHAG for PEM-5 (7 ± 2 PHAG) compared to that for PEM-6 (2 ± 1 PHAG) was already evident from the FTIR spectra above. As was already mentioned above, preferential binding of the PHAG to the PEM-5 occurs via electrostatic interactions between the cationic surface charge of the outermost PEI layer and the negative net charge of the PHAG, where the negative net charge of the PHAG is assumed to be originated preferentially by anionic patches of the coat proteins of the capsid layer.[27] The lower binding of PHAG at PEM-6 (outermost DAC layer) might originate from the respective electrostatic repulsion.

In Vitro Antibacterial Testing. Antibacterial tests were performed on agar plates, at which either PEM coatings (PEI/DAC) without PHAG or PEM coatings with PHAG were deposited and afterward infected with *S. aureus* bacteria (for details, see Experimental Methods). In Figure 8, photographic images of PEM- and PEM + PHAG-coated agar plates after infection with *S. aureus* bacteria are shown.

Qualitatively, the turbid appearance of the infected agar plates indicates bacterial growth and colonization, while clear regions or spots (plaques) on the agar plates indicate eradication of the bacteria by PHAG-originated lysis. Quantitatively, the clearance of the area can be evaluated and taken as a measure for strength and amount of PHAG binding as well as for subsequent inhibition of bacterial growth (see Experimental Methods).

First of all, the negative control experiment (Figure 8a) shows no bacterial eradication for agar plates treated neither by PEM nor by PHAG, while the positive control experiment (Figure 8b) shows significant bacterial eradication for agar plates treated by PHAG. Quantitative image analysis revealed around 47 ± 9% of eradication.

Second, for agar plates coated with pure PEM-5 and PEM-6, both in the absence of PHAG Figure 8c,e show undisturbed *S. aureus* bacterial growth by remaining turbidity, which can be quantitatively expressed by image analysis as 0% of eradication.

Third, in contrast, for the agar plates coated with PEM-5 + PHAG and PEM-6 + PHAG, both modified by PHAG clearly extended regions and spots (plaques) were observed in Figure 8d,f, indicating bacterial eradication. Quantitative image analysis revealed that the degree of eradication is lower for the agar plates coated with PEM-5 + PHAG (23 ± 12%) when compared to PEM-6 + PHAG (79 ± 14%). In other words, significantly, PEM-6 + PHAG ranges above and PEM-5 + PHAG ranges below the value of the negative control (47 ± 9%). This result was unexpected since from the spectroscopic and microscopic PHAG binding studies reported above, significantly more PHAG appeared to be bound at PEM-5 when compared to PEM-6, as provided in Table 1.

Table 1. Summarized Results of PHAG Binding and Antibacterial Effect of PEM (+PHAG) Coatings for the PEI/DAC System (Prepared with 0.1 M NaCl) Based on ATR-FTIR and AFM Data

PEI/DAC	PEM-5	PEM-6	PEM-5 + PHAG	PEM-6 + PHAG
amide I/II integral (ATR-FTIR)	---	---	0.926 ± 0.318	0.152 ± 0.112
number PHAG per 4 × 4 μm^2 (AFM)	---	---	7 ± 2	2 ± 1
in vitro (bacterial eradication, %)	0 ± 0	0 ± 0	23 ± 12	79 ± 14

Although both polyelectrolytes PEI[15] and DAC[16,17,29] are known for their inherent antibacterial properties, as they can rupture or form a physical barrier against the bacterial cell wall, both PEM-5 and PEM-6 without PHAG did not show bacterial eradication (see Table 1). Since both the pure outermost PEI (PEM-5) and DAC layer (PEM-6) have no significant antibacterial properties, the antibacterial properties of both PEM-5 + PHAG and PEM-6 + PHAG are clearly related to the presence of the PHAG. The more important reason for the different antibacterial effect of PEM-5 + PHAG and PEM-6 + PHAG could be the obvious different binding strengths of PHAG to the outermost PEI layer (PEM-5) when compared to the outermost DAC layer (PEM-6). Presumably, the lower attractive interaction of PHAG with the outermost DAC layer (PEM-6) allows better migration of PHAG within the agar/bacterium system. However, the higher attraction of PHAG to the outermost PEI layer (PEM-5) does not allow the migration of PHAG within the agar/bacterium system. Finally, nevertheless, it can be assumed that the PHAG is bound to the outermost PEM layer and is mainly responsible for the antibacterial effect.

The geometry in which the PHAG is bound to the PEM could also play a role in the effectiveness of the PEM + PHAG coatings. If PHAG is applied to a PEM-5 with a positive surface charge, it could potentially be bound to the PEM-5 in a "head down to substrate" configuration due to the attraction of the anionic head to the cationic PEM. When PHAG is bound to a PEM-6 with a negative surface charge, the PHAG could be bound in a more "tail bound to substrate" or "head exposed to ambient" configuration. Since PHAG infects bacteria by injection via their tail, the geometry of the PHAG-bond could influence the antibacterial activity. However, AFM measurements have not yet revealed any indications of the geometry of bound PHAG.

CONCLUSIONS

PEL multilayers (PEM) using cationic poly(ethylenimine) (PEI) and an anionic graft polymer from hyaluronic acid and poly(L-lactide) (DAC) were successfully generated as platforms to bind PHAG at model biomaterials. The ATR-FTIR spectra of PEM after contact with the PHAG suspension show that *S. aureus* PHAG can be attached to PEM. Here, a larger amount of PHAG could be bound to odd-numbered PEM if compared to even-numbered ones, as indicated by the stronger increase of characteristic IR bands of the PHAG. In addition, a greater number of PHAG bound to PEM-5 than to PEM-6 with typical head/tail architecture was observed in the AFM

https://doi.org/10.1021/acsomega.4c06933
ACS Omega 2024, 9, 49432−49440

images supporting the ATR-FTIR results. The preferred attachment to PEM-5 can be explained by the electrostatic interaction between the anionic capsid proteins of PHAG and the cationic terminating PEI layer of PEM-5.

In vitro tests with coated agar plates were performed to determine the antibacterial activity of the coatings. The PEM + PHAG samples (PEM-5 + PHAG, PEM-6 + PHAG) showed a general clear antibacterial effect (eradication: 23−79%) compared to the pure PEM samples (PEM-5, PEM-6: 0%). Although PEM-6 and PEM-5 coatings have shown lower and higher amounts of bound PHAG, respectively, antibacterial in vitro tests revealed that the coatings composed of PEM-6 + PHAG had significantly higher antibacterial activity than the coatings prepared from PEM-5 + PHAG. This result was unexpected but could be explained by the properties of the respective terminating layers of PEM-5 and PEM-6. Apparently, the antibacterial effect of the PEM-6 + PHAG coating is higher than that of the PEM-5 + PHAG coating, although more PHAG is bound to PEM-5. Presumably, it is the weaker interaction between PEM-6/PHAG compared to PEM-5/PHAG, which allows PHAG to migrate within the agar/bacterium system or to be released in higher amounts from the coating and to act against planktonic bacteria in the bulk phase.

Finally, the production of PHAG-loaded antibacterial PEM coatings appears to be very efficient. On the one side, the antibacterial coating serves for a limited initial bacterial attachment in the sense of impeding the "race for the surface".[5,6] On the other side, PHAG may infect those host bacteria, which already succeeded in initial attachment and replication, transcript, and translate therein to new PHAG, which also could eliminate both sessile and planktonic bacteria. Hence, the PHAG-based antibacterial therapy addresses those bacteria, which either still compete or already have won the race for the surface. Further studies are necessary to elucidate the lytic action of PEM bound to PHAG.

■ ASSOCIATED CONTENT

Supporting Information

The Supporting Information is available free of charge at https://pubs.acs.org/doi/10.1021/acsomega.4c06933.

Additional AFM images on PEM of PEI/DAC without and with bound PHAG in the absence and presence of salt (PDF)

■ AUTHOR INFORMATION

Corresponding Author

Martin Müller − *Leibniz-Institut für Polymerforschung Dresden e.V., 01069 Dresden, Germany; Technische Universität Dresden, 01062 Dresden, Germany;* orcid.org/0000-0001-8961-4604; Email: mamuller@ipfdd.de

Authors

Luise Wirth − *Leibniz-Institut für Polymerforschung Dresden e.V., 01069 Dresden, Germany; Technische Universität Dresden, 01062 Dresden, Germany*

Birgit Urban − *Leibniz-Institut für Polymerforschung Dresden e.V., 01069 Dresden, Germany*

Eva Bittrich − *Leibniz-Institut für Polymerforschung Dresden e.V., 01069 Dresden, Germany;* orcid.org/0000-0003-1484-1786

Gopala-Krishna Mannala − *Universitätsklinikum Regensburg, 93053 Regensburg, Germany*

Volker Alt − *Universitätsklinikum Regensburg, 93053 Regensburg, Germany*

Complete contact information is available at: https://pubs.acs.org/10.1021/acsomega.4c06933

Author Contributions

L.W.: Conceptualization, investigation, methodology, writing original draft, reviewing, and editing; B.U.: Methodology and investigation; E.B.: Methodology and writing; G.-K.M.: Conceptualization, investigation, methodology, writing, reviewing, and editing; V.A.: Funding acquisition, supervision, conceptualization, and writing; M.M.: Funding acquisition, supervision, conceptualization, methodology, writing, reviewing, and editing.

Notes

The authors declare no competing financial interest.

■ ACKNOWLEDGMENTS

This work was funded by Deutsche Forschungsgemeinschaft (DFG, PN 491 517 909).

■ ABBREVIATIONS

DAC:defensive antibacterial coating; IAI:implant-associated infections; MRSA:methicillin-resistant *Staphylococcus aureus*; PEI:poly(ethylenimine); PEM:polyelectrolyte multilayer; PFU:plaque-forming units; PHAG:bacteriophages; S. aureus:-*Staphylococcus aureus*

■ REFERENCES

(1) Kaźmierczak, Z.; Górski, A.; Dabrowska, K. Facing antibiotic resistance: Staphylococcus aureus phages as a medical tool. *Viruses* **2014**, *6* (7), 2551−2570.

(2) Murray, C. J. L.; Ikuta, K. S.; Sharara, F.; Swetschinski, L.; Robles Aguilar, G.; Gray, A.; Han, C.; Bisignano, C.; Rao, P.; Wool, E.; Johnson, S. C.; Browne, A. J.; Chipeta, M. G.; Fell, F.; Hackett, S.; Haines-Woodhouse, G.; Kashef Hamadani, B. H.; Kumaran, E. A. P.; McManigal, B.; Naghavi, M.; et al. Global burden of bacterial antimicrobial resistance in 2019: A systematic analysis. *Lancet* **2022**, *399* (10325), 629−655.

(3) Klevens, R. M.; Morrison, M. A.; Nadle, J.; Petit, S.; Gershman, K.; Ray, S.; Harrison, L. H.; Lynfield, R.; Dumyati, G.; Townes, J. M.; Craig, A. S.; Zell, E. R.; Fosheim, G. E.; Mcdougal, L. K.; Carey, R. B.; Fridkin, S. K. (n.d.). Invasive methicillin-resistant staphylococcus aureus infections in the United States. *JAMA* **2007**, *298* (15), 1763−1771.

(4) Zhuang, Y.; Ren, L.; Zhang, S.; Wei, X.; Yang, K.; Dai, K. Antibacterial effect of a copper-containing titanium alloy against implant-associated infection induced by methicillin-resistant Staphylococcus aureus. *Acta Biomater.* **2021**, *119*, 472−484.

(5) Seebach, E.; Kubatzky, K. F. Chronic implant-related bone infections - Can immune modulation be a therapeutic strategy? *Front. Immunol.* **2019**, *10*, No. 1724.

(6) Gristina, A. G. Biomaterial-Centered Infection: Microbial Adhesion Versus Tissue Integration. *Science* **1987**, *237* (4822), 1588−1595.

(7) Bürgers, R.; Hahnel, S.; Rosentritt, M.; Handel, G. Biofilmbildung auf dentalen Implantatoberflächen. *ZWR* **2010**, *119* (5), 244−252.

(8) Abedon, S. T.; Kuhl, S. J.; Blasdel, B. G.; Kutter, E. M. Phage treatment of human infections. *Bacteriophage* **2011**, *1* (2), 66−85.

(9) Herelle, F. D. Sur un microbe invisible antagoniste des bacilles dysentériques. *C. R. Acad. Sci.* **1917**, *165*, 373−375.

(10) Müller, M.; Urban, B.; Mannala, G. K.; Alt, V. Poly-(ethyleneimine)/poly(acrylic acid) multilayer coatings with peripherally bound Staphylococcus aureus bacteriophages have antibacterial properties. *ACS Appl. Polym. Mater.* **2021**, *3* (12), 6230−6237.
(11) Yang, S. H.; Chung, W. J.; McFarland, S.; Lee, S. W. Assembly of bacteriophage into functional materials. *Chem. Rec.* **2013**, *13* (1), 43−59.
(12) Decher, G.; Eckle, M.; Schmitt, J.; Struth, B. Layer-by-layer assembled multicomposite films. *Curr. Opin. Colloid Interface Sci.* **1998**, *3* (1), 32−39.
(13) Petrila, L. M.; Bucatariu, F.; Mihai, M.; Teodosiu, C. Polyelectrolyte multilayers: An overview on fabrication, properties, and biomedical and environmental applications. *Materials* **2021**, *14* (15), 4152.
(14) Mannala, G. K.; Rupp, M.; Walter, N.; Brunotte, M.; Alagboso, F.; Docheva, D.; Brochhausen, C.; Alt, V. Microbiological and ultrastructural evaluation of bacteriophage 191219 against planktonic, intracellular and biofilm infection with Staphylococcus aureus. *Eur. Cells Mater.* **2022**, *43*, 66−78.
(15) Gibney, K. A.; Sovadinova, I.; Lopez, A. I.; Urban, M.; Ridgway, Z.; Caputo, G. A.; Kuroda, K. Poly(ethylene imine)s as antimicrobial agents with selective activity. *Macromol. Biosci.* **2012**, *12* (9), 1279−1289.
(16) Pressato, D.; Battista, A.; Govoni, M.; Vivarelli, L.; Dallari, D.; Pellegrini, A. The intraoperative use of defensive antibacterial coating (DAC) in the form of a gel to prevent peri-implant infections in orthopaedic surgery: A clinical narrative review. *Materials* **2023**, *16* (15), 5304.
(17) Gaetano, G.; Pitarresi, G.; Palumbo, F. S.; Maraldi, S.; Scarponi, S.; Romano, C. L.Hyaluronic-based antibacterial hydrogel coating for implantable biomaterials in orthopedics and trauma: From basic research to clinical applications. In *Hydrogels*; IntechOpen, 2018; pp 180−190.
(18) Müller, M.; Rieser, T.; Lunkwitz, K.; Meier-Haack, J. Polyelectrolyte complex layers: A promising concept for antifouling coatings verified by in-situ ATR-FTIR spectroscopy. *Macromol. Rapid Commun.* **1999**, *20* (12), 607−611.
(19) Harrick, N. J. *Internal Reflection Spectroscopy*; Harrick Scientific Corp.: Ossining, NY, USA, 1979.
(20) Reviakine, I.; Johannsmann, D.; Richter, R. P. Hearing what you cannot see and visualizing what you hear: Interpreting quartz crystal microbalance data from solvated interfaces. *Anal. Chem.* **2011**, *83* (23), 8838−8848.
(21) Sauerbrey, G. Verwendung von Schwingquarzen zur Wägung dünner Schichten und zur Mikrowägung. *Z. Phys.* **1959**, *155*, 206−222.
(22) Decher, G.; Hong, J. D.; Schmitt, J. Buildup of ultrathin multilayer films by a self-assembly process. III. Consecutively alternating adsorption of anionic and cationic polyelectrolytes on charged surfaces. *Thin Solid Films* **1992**, *210*−*211*, 831−835.
(23) Alince, B.; Vanerek, A.; Van de Ven, T. G. M. Effect of Surface Topography, pH and Salt on the Adsorption of Polydisperse Polyethylenimine onto Pulp Fibers, Berichte der Bunsengesellschaft für physikalische. *Chemie* **1996**, *100* (6), 954−962.
(24) Dubas, S. T.; Schlenoff, J. B. Factors Controlling the Growth of Polyelectrolyte Multilayers. *Macromolecules* **1999**, *32* (24), 8153−8160.
(25) Müller, M. The anomalous influence of polyelectrolyte concentration on the deposition and nanostructure of poly-(ethyleneimine)/poly(acrylic acid) multilayers. *Molecules* **2019**, *24* (11), 2141.
(26) Heffron, J.; Mayer, B. K. Virus isoelectric point estimation: Theories and methods. *Appl. Environ. Microbiol.* **2021**, *87* (3), e02319.
(27) Archer, M. J.; Liu, J. L. Bacteriophage T4 nanoparticles as materials in sensor applications: Variables that influence their organization and assembly on surfaces. *Sensors* **2009**, *9* (8), 6298−6311.
(28) Das, B. P.; Tsianou, M. From polyelectrolyte complexes to polyelectrolyte multilayers: Electrostatic assembly, nanostructure, dynamics, and functional properties. *Adv. Colloid Interface Sci.* **2017**, *244*, 71−89.
(29) Pitarresi, G.; Palumbo, F. S.; Calascibetta, F.; Fiorica, C.; di Stefano, M.; Giammona, G. Medicated hydrogels of hyaluronic acid derivatives for use in orthopedic field. *Int. J. Pharm.* **2013**, *449* (1−2), 84−94.

https://doi.org/10.1021/acsomega.4c06933
ACS Omega 2024, 9, 49432−49440